JACS
JOURNAL OF THE AMERICAN CHEMICAL SOCIETY

Communication

Structural and Spectroscopic Characterization of an Electrophilic Iron Nitrido Complex

Jeremiah J. Scepaniak, Meita D. Fulton, Ranko P. Bontchev, Eileen N. Duesler, Martin L. Kirk, and Jeremy M. Smith

J. Am. Chem. Soc., **2008**, 130 (32), 10515-10517 • DOI: 10.1021/ja8027372 • Publication Date (Web): 17 July 2008

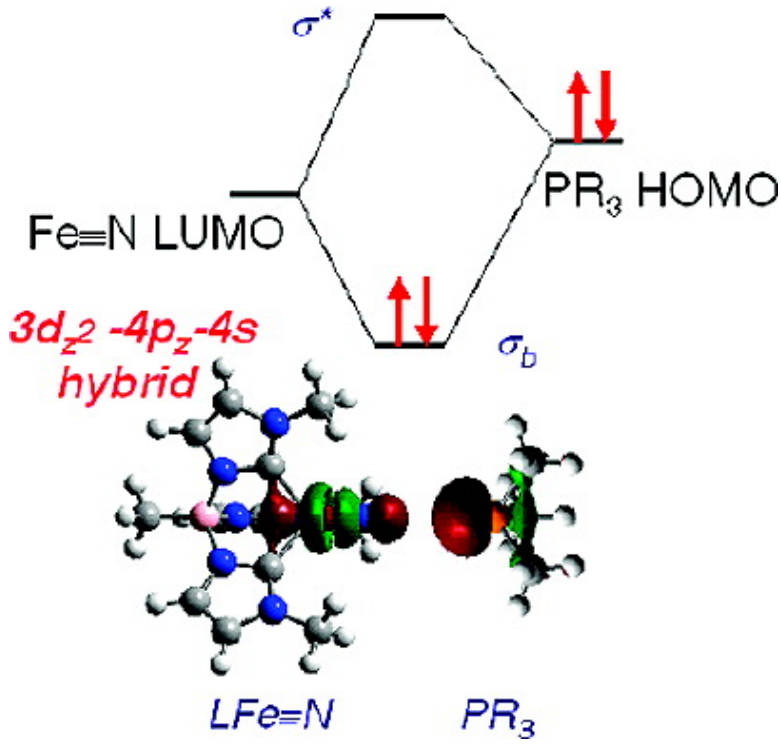

More About This Article

Additional resources and features associated with this article are available within the HTML version:

- Supporting Information
- Access to high resolution figures
- Links to articles and content related to this article
- Copyright permission to reproduce figures and/or text from this article

J|A|C|S
COMMUNICATIONS

Published on Web 07/17/2008

Structural and Spectroscopic Characterization of an Electrophilic Iron Nitrido Complex

Jeremiah J. Scepaniak,[†] Meita D. Fulton,[§] Ranko P. Bontchev,[‡] Eileen N. Duesler,[§] Martin L. Kirk,*[,§] and Jeremy M. Smith*[,†]

Department of Chemistry and Biochemistry, New Mexico State University, Las Cruces, New Mexico 88003, Cabot Corporation, 5401 Venice Avenue NE, Albuquerque, New Mexico 87113, and Department of Chemistry and Chemical Biology, The University of New Mexico, Albuquerque, New Mexico 87131

Received April 14, 2008; E-mail: jesmith@nmsu.edu; mkirk@unm.edu

Nitrido ligands are important species in the activation of N_2 by transition metal complexes. For example, molybdenum nitrides are produced by the reductive cleavage of N_2[1] and are also implicated in the catalytic reduction of N_2 to NH_3.[2] Nitrido ligands also find application in nitrogen atom transfer reactions,[3] the most notable of which utilize N_2 as the nitrogen atom source.[4] Finally, nitrido complexes may also serve as precursors to C≡C and C≡N metathesis catalysts.[5]

Iron nitrido complexes are of interest due to their relevance as potential models for nitrogen fixation by the nitrogenase metalloenzyme.[6] The reactivity of iron nitrido complexes is also of fundamental interest. Late metal nitrido complexes often display electrophilic reactivity,[7,8] in contrast to the nucleophilic behavior of nitrido ligands in early to mid-transition metal complexes.[7]

Few iron complexes containing terminal nitrido ligands have been reported. Octahedral iron(V) and iron(VI) nitridos supported by heme and non-heme ligands can be prepared in frozen matrices by photolysis of precursor azido complexes.[9,10] Iron(IV) nitrido complexes supported by tris(phosphino)borate ligands can be generated in solution at room temperature, although they cannot be isolated.[11,12] The crystallographic characterization of $[(TIMEN^R)Fe{\equiv}N]^+$ iron(IV) nitrido complexes, which are supported by bulky and flexible tris(carbene)amine ligands, has recently been reported.[13]

In this contribution, we report the synthesis and characterization of an iron nitrido complex supported by the phenyltris(1-*tert*-butylimidazol-2-ylidene)borate (L^{tBu-}) ligand. Structural and spectroscopic characterization of this complex has allowed us to determine its detailed electronic structure. The electrophilic character of the nitrido ligand has been characterized through its reactivity with triarylphosphines.

The four-coordinate iron(II) chloride complex $L^{tBu}FeCl$ is prepared from "$PhB(^tBuIm)_3^-$" and $FeCl_2(THF)_{1.5}$, similarly to the synthesis of $L^{tBu}CoCl$.[14] Reaction of this complex with NaN_3 leads to the formation of a new complex that has been formulated as $L^{tBu}Fe{-}N{=}N{=}N$ on the basis of its ^1H NMR and IR spectra ($\nu_{N=N=N} = 2081\ cm^{-1}$). Irradiation of this colorless complex results in quantitative formation of the orange-red nitrido complex $L^{tBu}Fe{\equiv}N$ (**1**). This complex can also be prepared in a one-pot reaction by photolyzing a mixture of $L^{tBu}FeCl$ and NaN_3 in a quartz reaction vessel (Scheme 1).

The iron nitrido complex **1** has been characterized in the solid state by X-ray crystallography of crystals grown from acetonitrile (Figure 1). The complex adopts a pseudo-tetrahedral structure, with

Scheme 1. Synthesis of **1**

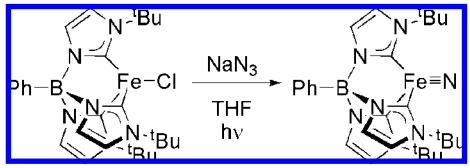

the nitrido ligand on the molecular threefold axis (B(1)−Fe(1)−N(1) angle = 178.57(6)°). The Fe−N bond of 1.512(1) Å is shorter than the Fe−N distances reported for the $[(TIMEN^R)Fe{\equiv}N]^+$ complexes (1.526(2) and 1.527(3) Å).[13] The Fe−N bond is 0.1 Å shorter than the Fe−N bond in our recently reported tris(carbene)borate iron(IV) imido complex.[15] Despite the apparent similarity of **1** and the tris(carbene)amine iron nitrido complexes, there are some significant structural differences. The $[(TIMEN^R)Fe{\equiv}N]^+$ complexes have C_3 symmetry with the iron atom ca. 0.4 Å out of the plane defined by the three carbene carbon atoms. In the case of C_{3v} symmetric **1**, the iron atom lies ca. 1 Å out of the plane defined by the three carbon atoms of the tris(carbene)borate ligand.

The NMR spectral data of **1** are consistent with the solid state structure and similar to related iron(IV) nitrido complexes.[11,13] Six signals are observed in the diamagnetic ^1H NMR spectrum, consistent with threefold symmetry in solution. The nitrido ligand was detected at δ 1019 ppm in the ^{15}N NMR spectrum of an isotopically enriched sample, which is similar to that observed for other iron(IV) nitrido complexes.[11,13]

The electronic absorption spectrum of **1** (Figure 2) in diethyl ether displays three distinct absorption maxima at 20 921 cm^{-1} (band 1; $\epsilon = 1230\ M^{-1}\ cm^{-1}$), 30 864 cm^{-1} (band 2; $\epsilon = 7292\ M^{-1}\ cm^{-1}$), and 37 736 cm^{-1} (band 3; $\epsilon = 8708\ M^{-1}\ cm^{-1}$). The extinction coefficient for band 1 is at the upper limit of that

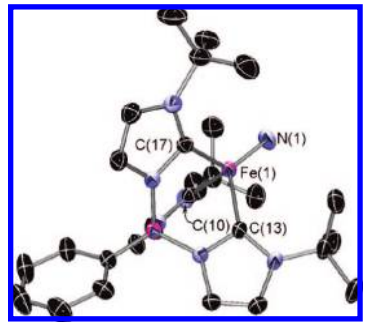

Figure 1. X-ray crystal structure of **1** with thermal ellipsoids at 50% probability. Selected bond lengths (Å) and angles (°): Fe(1)−N(1) 1.512(1); Fe−C(17) 1.915(1);Fe−C(3) 1.928(1); Fe−C(10) 1.928(1); C(17)−Fe-C(3) 96.35(5); C(17)−Fe-C(10) 97.90(5); C(3)−Fe-C(10) 94.44(5).

[†] New Mexico State University.
[‡] Cabot Corporation.
[§] The University of New Mexico.

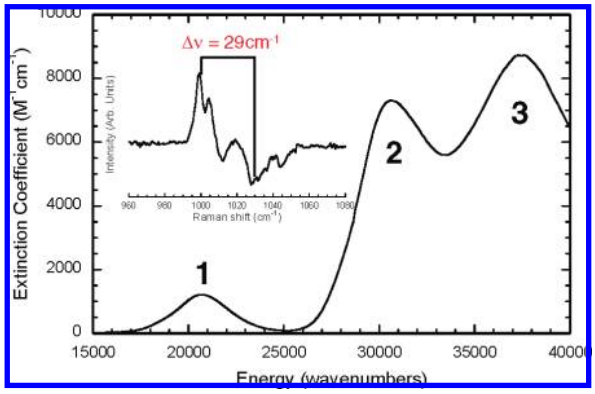

Figure 2. Solution electronic absorption spectrum of **1** in diethyl ether. Inset: Isotope edited solid state resonance Raman spectrum of **1** in NaCl. The $^{15}N-^{14}N$ difference spectrum was obtained by spectral subtraction to yield the best flat baseline from 900 to 1100 cm^{-1}. Positive features derive from the ^{15}N spectrum, and negative features from the ^{14}N spectrum.

anticipated for a ligand field transition in the non-centrosymmetric ligand field of **1**. Ligand field theory arguments coupled with the results of bonding calculations[16] strongly suggest a $d_{e(a)}{}^4$, $d_{a1}{}^0$, $d_{e(b)}{}^0$ electronic configuration for **1** in C_{3v} symmetry. Thus, four spin-allowed ligand field transitions are predicted from the $^1A_1$ ground state. The lowest energy transition is the *xy*-polarized $^1A_1 \rightarrow {}^1E$ which derives from a $e_{(a)} \rightarrow a_1$ one-electron promotion. Although this ($e_{(a)} \rightarrow a_1$) $^1A_1 \rightarrow {}^1E$ transition is dipole-allowed, it is overlap forbidden, and the intensity is predicted to be very weak due to the small ligand−ligand term in the expansion of the transition dipole moment integral.[17] This is confirmed by TDDFT calculations that also predict this transition to possess a very small oscillator strength ($\epsilon \sim 12\ M^{-1}\ cm^{-1}$). The $e_{(a)} \rightarrow e_{(b)}$ one-electron promotion yields $^1A_1$, $^1A_2$, and ^1E excited states, and the *z*-polarized $^1A_1 \rightarrow {}^1A_1$ transition is predicted to possess the highest oscillator strength. Therefore, band 1 is assigned as the $^1A_1 \rightarrow {}^1A_1$ LF transition ($e_{(a)} \rightarrow e_{(b)}$ one electron promotion). Both the intensity and higher energy of band 2 support a charge transfer assignment for this transition. This, coupled with the capability of the L'^{Bu} carbene ligand fragments to act as π-acceptors, indicates that band 2 is most likely a MLCT transition (Fe $d_{e(a)} \rightarrow$ carbene π^*), and this is supported by our TDDFT calculations. Band 3 is more complex and comprises multiple transitions with the intensity likely arising from dominant Fe $d_{e(a)} \rightarrow$ carbene charge transfer character.

Inspection of the $e_{(b)}$ isodensity surfaces (Figure 3) and analysis of the overlap populations[18] indicate that the Fe≡N interaction is antibonding while the Fe−$C_{carbene}$ interaction is weakly bonding in the $e_{(b)}$ MO. Since $e_{(a)}$ is essentially Fe−$C_{carbene}$ nonbonding, we can predict that one-electron promotions from $e_{(a)}$ to $e_{(b)}$ should result in appreciable distortions along totally symmetric Fe≡N and Fe−C_3 vibrational modes. Upon excitation into band 1, low-frequency Raman bands at 328, 398, 448, and 536 cm^{-1} are resonantly enhanced and assignable as totally symmetric Fe(C_3N_3B) core vibrations. Interestingly, these subtract out completely in the isotope-edited spectra, indicating that these totally symmetric core modes are not coupled or mixed with the Fe≡N stretch. Additional support for the lack of mode mixing between "in-plane" Fe−C_3 modes and the "out-of-plane" Fe≡^{14}N stretch derives from the observed shift in the Fe≡N stretch upon isotopic substitution (Figure 2, inset); the 1028 cm^{-1} Fe≡^{14}N stretch shifts to 999 cm^{-1} upon ^{15}N substitution ($\Delta\nu = 28\ cm^{-1}$ for diatomic Fe≡N).

The unusual nature of the Fe a_1 orbital has been previously noted.[12,19] This orbital is calculated to lie at a lower energy than the $e_{(b)}$ orbital set despite an anticipated strong Fe(d_{z^2})−N(p_z) antibonding interaction. Here, we present two key factors that may account for the low energy of this a_1 orbital. The first is directly related to the N−Fe−C bond angle which places the Fe−C bond very close to the Fe(d_{z^2}) nodal plane, significantly reducing Fe−C σ-type interactions with the Fe(d_{z^2}) orbital. Thus, the primary ligand interaction with Fe(d_{z^2}) involves only the terminal nitrido. Interestingly, the overlap population analysis[18] for **1** indicates that the a_1 Fe(d_{z^2})−N(p_z) interaction possesses a reduced net overlap. For this to be true, the equatorial (−) component of the Fe(d_{z^2}) orbital must have considerable positive overlap with the (−) N(p_z) lobe while the axial (+) lobe of the Fe(d_{z^2}) orbital must have reduced negative overlap with the (−) N(p_z) lobe (Figure 3B). This could occur upon formation of a dsp hybrid orbital from Fe s, p_z, and d_{z^2} orbitals. Here, admixed s orbital character would increase the radial distribution of the equatorial (−) component of the Fe(d_{z^2}) orbital, while a properly phased Fe $4p_z$ orbital mixing would reduce the axial lobe in the direction of the nitrido ligand and increase the axial lobe opposite the Fe≡N bond (Figure 3B). Evidence for Fe ($3d_{z^2}$)−($4p_z$) configurational mixing (Figure 3C) derives from the very intense pre-edge transition in the Fe K-edge spectrum of a related C_{3v} Fe nitrido complex.[12] A key manifestation of this strong Fe ($3d_{z^2}$)−($4p_z$) configurational mixing is the stabilization of the Fe a_1 orbital of $3d_{z^2}$ parentage. This is important since symmetry and steric constraints dictate that the Fe $3d_{z^2}$ orbital is the acceptor orbital in two-electron atom transfer reactions with PR_3-type nucleophiles. Thus, configurational mixing in **1** allows for stabilization of the Fe $3d_{z^2}$ orbital, and this is expected to facilitate reactions with nucleophiles.

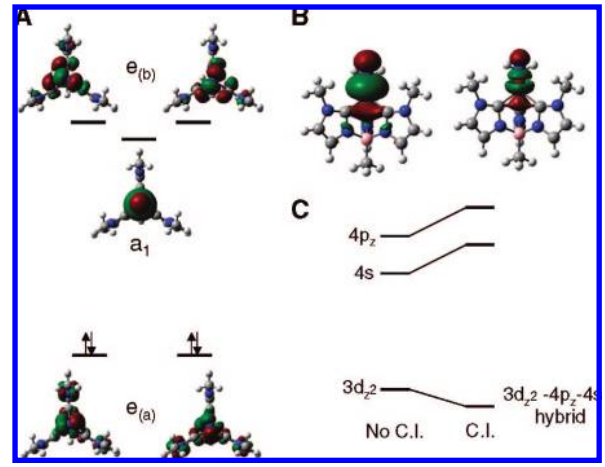

Figure 3. (A) Isodensity surfaces for the five Fe 3d-based molecular orbitals of $e_{(a)}$, a_1, and $e_{(b)}$ symmetry (0.04 cutoff). The view is looking down the N≡Fe bond (C_3 axis). (B) Alternative views of the a_1 orbital at different isodensity values (0.04, left; 0.06, right). (C) Diagram indicating how virtual Fe 4s and $4p_z$ orbitals of a_1 symmetry might stabilize the Fe $3d_{z^2}$ a_1 orbital.

Our understanding of the electronic structure of **1** has prompted us to investigate the reactivity of the iron nitrido group toward phosphines. We find that **1** reacts slowly with triphenylphosphine to form the orange phosphiniminato complex L'^{Bu}Fe−N=PPh_3 (**2**) in high yield. This complex has also been crystallographically characterized (Figure 4).[20] The Fe(1)−N(1) bond length (1.894(2) Å) is significantly longer than that in **1** and similar to Fe−N bond lengths observed in low coordinate iron amido complexes.[21] The very short P(1)=N(1) bond (1.527(2) Å), which is shorter than that in $(Ph_3PNLi)_6(THF)_5$,[22] is consistent with its formulation as a double bond.[23] The Fe−C bond lengths increase by ca. 0.2 Å from **1**, causing the iron atom to be further out of the plane defined by the carbene carbons (ca. 1.2 Å). In solution, **2** displays a paramagneti-

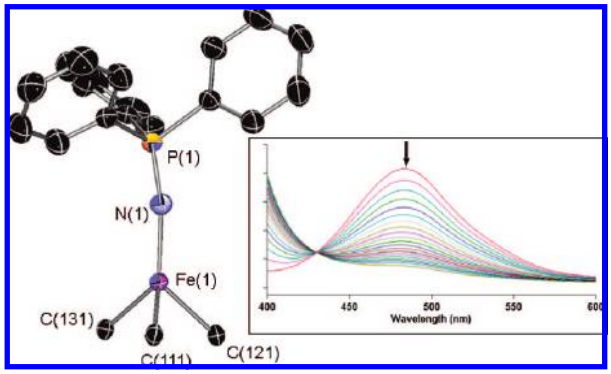

Figure 4. X-ray crystal structure of **2**. One of two molecules in the asymmetric unit shown. Thermal ellipsoids at 50% probability, most of the tris(carbene)borate ligand, hydrogen atoms, and solvent molecules are omitted for clarity. Selected bond lengths (Å) and angles (°): Fe(1)−N(1) 1.894(2); Fe−C(111) 2.102(2); Fe(1)−C(121) 2.137(2); Fe(1)−C(131) 2.151(2);N(1)−P(1)1.527(2);C(111)−Fe(1)−C(121)87.76(8);C(111)−Fe(1)−C(131) 92.83(8); C(121)−Fe(1)−C(131) 87.85(8) Fe(1)−N(1)−P(1) 167.8(1). Inset: Spectral evolution of the reaction between **1** (initial concentration = 0.57 mM) and PPh_3 (0.40 M) in THF at 299 K. Traces are shown at 10 min intervals.

cally shifted ^{1}H NMR spectrum that is consistent with **2** having threefold symmetry in solution. The room-temperature solution magnetic moment of **2** is 5.0(3) BM; consistent with an $S = 2$ iron(II) species. The reaction of **1** and PPh_3, which involves attack of PPh_3 on the electrophilic nitrido ligand, can be described as nitrogen atom transfer from iron to the phosphine.[8a]

A tight isosbestic point is observed when the reaction of **1** with PPh_3 is monitored by UV−vis spectroscopy (Figure 4, inset). Measuring the rate of reaction under pseudo-first-order conditions reveals first-order behavior for both **1** and PPh_3, corresponding to the rate law, rate $= k_2[\mathbf{1}][PPh_3]$. The second-order rate constant at 299 K is $k_2 = (4.0 \pm 0.2) \times 10^{-4}$ M^{-1} s^{-1}. Analysis of the temperature dependence of the rate constant gives activation parameters for this reaction of $\Delta H^{\ddagger} = 13.7 \pm 0.1$ kcal/mol and $\Delta S^{\ddagger} = -30 \pm 1$ e.u. (284−329 K). Nitrogen atom transfer from iron to phosphorus therefore occurs by an associative mechanism.[24] The kinetic results are consistent with a reaction mechanism involving nucleophilic attack of triphenylphosphine (HOMO) at the electrophilic nitrido ligand of **1** (a_1 LUMO) and provides support for the electronic structure described above.

In summary, we have isolated and structurally characterized a terminal iron nitrido complex **1** supported by a bulky tris(carbene)borate ligand. The electronic structure of **1** reveals that the a_1 LUMO (formerly Fe(d_{z^2})) is stabilized by spd mixing, and this unusual bonding interaction results in a nitrido ligand that has electrophilic character. Finally, this bonding description is supported by the reaction of **1** with PPh_3, which results in nitrogen atom transfer the phosphine, leading to **2**.

Acknowledgment. J.M.S. acknowledges funding from NMSU and the ACS-PRF. Support of this research by the National Institutes of Health (Grant No. GM-057378 to M.L.K.) is gratefully acknowledged. We thank Dennis L. Johnson for recording the ^{15}N NMR spectrum. and Ryan E. Cowley for obtaining the crystal structure of L$^{t\mathrm{Bu}}$FeCl. The Bruker X8 X-ray diffractometer was purchased via an NSF CRIF:MU award to The University of New Mexico, CHE-0443580.

Supporting Information Available: Complete experimental details and CIF files. This material is available free of charge via the Internet at http://pubs.acs.org.

References

(1) (a) Laplaza, C. E.; Cummins, C. C. *Science* **1995**, *268*, 861. (b) Cummins, C. C. *Chem. Commun.* **1998**, 1777.
(2) (a) Yandulov, D. V.; Schrock, R. R. *Science* **2003**, *301*, 76. (b) Schrock, R. R. *Acc. Chem. Res.* **2005**, *38*, 955.
(3) Selected examples: (a) Du Bois, J.; Hong, J.; Carreira, E. M.; Day, M. W. *J. Am. Chem. Soc.* **1996**, *118*, 915. (b) Bendix, J. *J. Am. Chem. Soc.* **2003**, *125*, 13348.
(4) (a) Henderickx, H.; Kwekkenbos, G.; Peters, A.; van der Spoel, J.; de Vries, K. *Chem. Commun.* **2003**, 2050. (b) Figueroa, J. S.; Piro, N. A.; Clough, C. R.; Cummins, C. C. *J. Am. Chem. Soc.* **2006**, *128*, 940. (c) Curley, J. J.; Sceats, E. L.; Cummins, C. C. *J. Am. Chem. Soc.* **2006**, *128*, 14036.
(5) (a) Chisholm, M. H.; Delbridge, E. E.; Kidwell, A. R.; Quinlan, K. B. *Chem. Commun.* **2003**, 126. (b) Gdula, R. L.; Johnson, M. J. A.; Ockwig, N. W. *Inorg. Chem.* **2005**, *44*, 9140. (c) Gdula, R. L.; Johnson, M. J. A. *J. Am. Chem. Soc.* **2006**, *128*, 9614. (d) Geyer, A. M.; Gdula, R. L.; Wiedner, E. S.; Johnson, M. J. A. *J. Am. Chem. Soc.* **2007**, *129*, 3800.
(6) (a) Einsle, O.; Tezcan, F. A.; Andrade, S. L. A.; Schmid, B.; Yoshida, M.; Howard, J. B.; Rees, D. C. *Science* **2002**, *297*, 1696. (b) Barney, B. M.; Lee, H.-I.; Dos Santos, P. C.; Hoffman, B. M.; Dean, D. R.; Seefeldt, L. C. *Dalton Trans.* **2006**, 2277.
(7) (a) Nugent, W. A.; Mayer, J. M. *Metal-Ligand Metal Multiple Bonds*; John Wiley & Sons: New York, 1988. (b) Eikey, R. A.; Abu-Omar, M. M. *Coord. Chem. Rev.* **2003**, *243*, 1.
(8) Selected examples: (a) Bakir, M.; White, P. S.; Dovletoglou, A.; Meyer, T. J. *Inorg. Chem.* **1991**, *30*, 2835. (b) Brown, S. N. *J. Am. Chem. Soc.* **1999**, *123*, 7459. (c) Crevier, T. J.; Bennett, B. K.; Soper, J. D.; Bowman, J. A.; Dehestani, A.; Hrovat, D. A.; Lovell, S.; Kaminsky, W.; Mayer, J. M. *J. Am. Chem. Soc.* **2001**, *123*, 1059. (d) Man, W.-L.; Lam, W. W. Y.; Yiu, S.-M.; Lau, T.-C.; Peng, S.-M. *J. Am. Chem. Soc.* **2004**, *126*, 15336.
(9) Nakamoto, K. *Coord. Chem. Rev.* **2002**, *226*, 153.
(10) (a) Meyer, K.; Bill, E.; Mienert, B.; Weyhermueller, T.; Wieghardt, K. *J. Am. Chem. Soc.* **1999**, *121*, 4859. (b) Aliaga-Alcalde, N.; DeBeer, G. S.; Mienert, B.; Bill, E.; Wieghardt, K.; Neese, F. *Angew. Chem., Int. Ed.* **2005**, *44*, 2908. (c) Berry, J. F.; Bill, E.; Bothe, E.; George, S. D.; Mienert, B.; Neese, F.; Wieghardt, K. *Science* **2006**, *312*, 1937.
(11) (a) Betley, T. A.; Peters, J. C. *J. Am. Chem. Soc.* **2004**, *126*, 6252. (b) Hendrich, M. P.; Genderson, W.; Behan, R. K.; Green, M. T.; Mehn, M. P.; Betley, T. A.; Lu, C. C.; Peters, J. C. *Proc. Natl. Acad. Sci. U.S.A.* **2006**, *103*, 17107.
(12) Rohde, J.-U.; Betley, T. A,.; Jackson, T. A.; Saouma, C. T.; Peters, J. C.; Que, L., Jr *Inorg. Chem.* **2007**, *45*, 5720.
(13) Vogel, C.; Heinemann, F. W.; Sutter, J.; Anthon, C; Meyer, K. *Angew. Chem., Int. Ed.* **2008**, *47*, 2681.
(14) Cowley, R. E.; Bontchev, R. P.; Duesler, E. N.; Smith, J. M. *Inorg. Chem.* **2006**, *45*, 9771.
(15) Nieto, I.; Ding, F.; Bontchev, R. P.; Wang, H.; Smith, J. M. *J. Am. Chem. Soc.* **2008**, *130*, 2716.
(16) *Gaussian 03*, revision C.02; Gaussian, Inc.: Pittsburgh, PA, 2003.
(17) (a) van der Avoird, A.; Ros, P. *Theor. Chim. Acta* **1965**, *4*, 13–21. (b) Mason, S. F. *Acc. Chem. Res.* **1979**, *12*, 55–61.
(18) Molecular orbitals were analyzed using the *AOMix* program. (a) Gorelsky, S. I. *AOMix: Program for Molecular Orbital Analysis*; York University: Toronto, 1997, http://www.sh-chem.net/. (b) Gorelsky, S. I.; Lever, A. B. P. *J. Organomet. Chem.* **2001**, *635*, 187–196.
(19) Tangen, E.; Conradie, J.; Ghosh, A. *J. Comput. Theory Comput.* **2007**, *3*, 448.
(20) Two molecules with similar metrical parameters are observed in the asymmetric unit. The major difference between these two molecules is the Fe−N−P angle (167.8(1) and 177.7(1)°), which is probably be due to packing forces in the solid state.
(21) (a) Eckert, N. A.; Smith, J. M.; Lachicotte, R. J.; Holland, P. L. *Inorg. Chem.* **2004**, *43*, 3306. (b) Betley, T. A.; Peters, J. C. *J. Am. Chem. Soc.* **2004**, *126*, 6252. (c) Eckert, N. A.; Vaddadi, S.; Stoian, S.; Lachicotte, R. J.; Cundari, T. R.; Holland, P. L. *Angew. Chem., Int. Ed.* **2006**, *45*, 6868.
(22) (a) Cristau, H. J.; Taillefer, M.; Rahier, N. *J. Organomet. Chem.* **2002**, *646*, 94. (b) Anfang, S.; Seybert, G.; Harms, K.; Geiseler, G.; Massa, W.; Dehnicke, K. *Z. Anorg. Allg. Chem.* **1998**, *624*, 1187.
(23) Dehnicke, K.; Krieger, M.; Massa, W. *Coord. Chem. Rev.* **1999**, *182*, 19.
(24) No significant electronic effect was observed for the reaction of L$^{t\mathrm{Bu}}$Fe≡N with a series of *para*-substituted triarylphosphines ($\rho = -0.04 \pm 0.03$ at 299 K). We suspect that steric interactions between the *tert*-butyl groups of the tris(carbene)borate ligand and the aryl groups of the phosphine are more important than the electronic differences between the phosphines in determining the rate of reaction.

JA8027372